

Assessing the vulnerability of overhead line wires to flashovers due to reduced insulation distances for power system resilience studies

Emanuele Ciapessoni
Energy Systems Development Dept.
Ricerca sul Sistema Energetico
RSE S.p.A.
Milan, Italy
emanuele.ciapessoni@rse-web.it

Diego Cirio
Energy Systems Development Dept.
Ricerca sul Sistema Energetico
RSE S.p.A.
Milan, Italy
diego.cirio@rse-web.it

Andrea Pitto
Energy Systems Development Dept.
Ricerca sul Sistema Energetico
RSE S.p.A.
Milan, Italy
andrea.pitto@rse-web.it

Silverio Casulli
Terna Corporate S.p.A.
Power System Planning Dept.
Rome, Italy
silverio.casulli@terna.it

Federico Falorni
Terna Corporate S.p.A.
Power System Planning Dept.
Rome, Italy
federico.falorni@terna.it

Francesca Scavo
Terna Corporate S.p.A.
Power System Planning Dept.
Rome, Italy
francesca.scavo@terna.it

Abstract— An accurate assessment of the vulnerability of power system components is a key pillar for long term resilience assessment studies and it helps prioritize the grid reinforcement interventions on the grid assets. Historical failure records indicate that neglecting the flashovers due to reduced insulation distances under specific conditions (wind-induced oscillations and increased sags) may affect the accuracy in the assessment of the overhead line vulnerability to threats, especially in presence of augmented sags due to vertical loads (wet snow). The paper proposes an analytical model to quantify the vulnerability of Overhead Lines (OHL) to flashover induced by reduced insulation distances, due to the combination of wire swinging conditions and moderate vertical loads. The model evaluates the conditional probability of OHL span flashover when subject to a specific vertical load, accounting for both geometric aspects (XYZ positions of the attachment points of the OHL wires) and electrical aspects (dependence of the dielectric distance on weather and orographic conditions). Tests on a set of lines in an area of the Italian transmission grid with frequent fault records due to such phenomena demonstrate the ability of the model to identify the most exposed lines and its good robustness to cope with uncertainties in the positions of the attachment points.

Index Terms – *flashover, overhead lines, resilience, vulnerability*.

I. INTRODUCTION

The increasing frequency and severity of extreme events due to climate changes calls for tools and methodologies able to support grid operators in deploying interventions aimed at improving the response of their systems to such extreme events [1]. In view of implementing effective resilience policies, Transmission System Operators (TSOs) need to assess the vulnerability of grid components. Currently, most techniques used to model the vulnerability of Overhead Lines (OHLs) against natural threats rely on statistical information on past failures [2][3]. Reference [4] lists some potential drawbacks and limitations of adopting statistical models, such as potential classification errors and the inability to model the potential benefits of hardening interventions. In the Italian Extra High Voltage (EHV) transmission system, wind and snow represent the two major causes of long-duration outages [5]. The ways how these threats affect the infrastructure are manifold: wind may cause the fall of objects (such as trees from outside the right of way) on the OHL wires and can

directly apply forces on the OHL subcomponents. On the other side, wet snow can either cause vertical loads on OHL subcomponents (shield wires, conductors, cross-arms) that can result in mechanical damages or in the reduction of subcomponents distance below the minimum clearance distance. An analytical model to account for these effects has been proposed in [4]. However, more complex phenomena may result in further flashovers with not negligible recovery times on the OHL spans: e.g. concurrent causes such as swinging wires due to moderate wind and increased sags due to additional vertical loads (such as due to wet snow accretion) can lead to reduced distances between energised wires (e.g. phase conductors) and mass/ground (shield wires or tower structure cross-arms). The variety of such phenomena would suggest the use of statistical models with the drawbacks already indicated. An accurate simulation of the dynamic behaviour of OHL wires during combined moderate wind conditions and wet snow loads requires the application of complex Finite Element Method (FEM) as the ones in [6] which are very computationally intensive. In [7] the authors propose a unified model with derived stability criterion to analyze the large swing of the overhead conductor under combined snow-wind conditions. The analytical model, solved by FEM with the aerodynamic coefficients obtained from simulated rain-wind tests, is able to capture the main features of the large swing of overhead conductor. All these models, however, would be very time consuming for extensive resilience assessment analyses on large power systems. Thus, a tradeoff must be pursued between model accuracy and speed of execution.

To cope with this gap, the present paper proposes an analytical model to assess OHL vulnerability under combined moderate wind conditions and wet snow loads, accounting for little information regarding the environment around the OHL span and the geometrical position of the attachment points of the OHL wires available in TSO databases.

The paper is organised as follows: Section II proposes the analytical model after a brief overview on the underlying physical phenomenon. Section III describes the case study on a small set of lines in a particularly exposed portion of the Italian transmission grid; moreover, it discusses the results obtained from the model, comparing its outcomes with the statistics from the recorded faults. Section IV concludes.

II. THE PROPOSED VULNERABILITY MODEL

This section describes the physical phenomenon underlying the analysed threat, namely the flashovers due to reduced insulation distances, and presents the proposed model for vulnerability assessment of the OHLs.

A. The underlying physical phenomena

Minimum clearance distances between energized parts (e.g. phase conductors) and grounded internal parts of the OHL (e.g. shield wires, cross arms) or external objects (roads, buildings etc.) are established by international and national standards [8][9], where these distances are calculated under “standard” operating conditions (e.g. at maximum sag temperature or predefined wind and snow loads). However, these conditions often do not correspond to actual operating conditions. Under real conditions, OHL insulation distances may not satisfy the minimum requirements to avoid high flashover probabilities due to the potential concurrence of several factors:

1. The presence of -even moderate- wind speeds causing large swingings in the OHL wires,
2. the presence of “increased sags” due to vertical loads e.g. for wet snow accumulation (see Figure 1),
3. the presence of lines at relatively lower HV levels (e.g. 60 kV), designed decades ago with criteria adequate for grid areas conventionally not considered “exposed” to snow events.

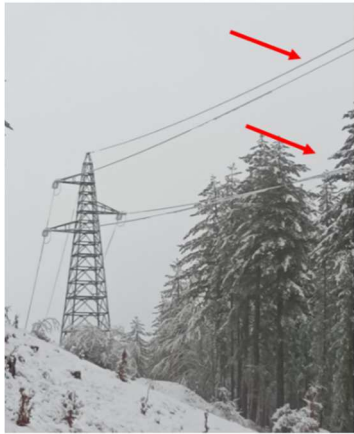


Figure 1. Increased sags due to vertical loads for wet snow accumulation on phase conductors and shield wires.

It's worth noting that the variety of factors concurring to the faults makes it difficult to understand the actual sequences of events during specific failures, because repair crews arrive at the failure site when initiating causes have already extinguished. In the end, all this requires careful post-processing of fault recordings in order to avoid errors in fault classification. However, according to TERNA statistics, the load disruptions following these faults can also take many hours to be solved, which represents an important aspect to be tackled in power system resilience analyses. In fact, this phenomenon caused a total ENS of around 2500 MWh in the Italian grid considering around 1000 events between 2012 and 2021.

B. Overview of the model

The proposed vulnerability model aims to model the vulnerability of the wires (i.e. phase conductors and shield wires) of each OHL span to reduced flashover distances due

to the concurrence of the abovementioned factors (moderate wind induced swingings, lower HV voltage design criteria, even moderate wet snow events). This model must take into account both geometrical aspects (i.e. the spatial configuration of the OHL wires) and environmental factors (i.e. orography of terrain, wet snow and wind speed and temperature conditions).

The model consists in two main parts (implemented as two different modules):

1. a probabilistic model of the Critical Flashover Voltage (CFO) representing the peak value of the voltage at industrial frequency, associated to a 50% probability of flashover, given a specific configuration of distances between energized wires (phase conductors) or between energized wires and shield wires; the model accounts for environmental conditions (temperature, air pressure, etc.),
2. a vulnerability model of each OHL span assessing the conditional failure probability of each span at specified wet snow loads, by evaluating the CFO probabilistic model at low clearance distances between phase conductors or between phases and shield wires, derived from the geometrical configuration of the swinging wires and the snow accumulated on the wires themselves.

The sequel of the section describes each module.

C. Probabilistic model for the 50% flashover voltage

International standards [8] provide indications to evaluate (both internal and external) minimum clearance distances on the basis of the type of the voltage waveforms (fast front, 50 Hz industrial, slow front). In particular, this paper focuses on flashovers in presence of industrial frequency voltage waveforms; thus, the maximum voltage U_{max} to which the system is subject is $\sqrt{2}U_{nom}/\sqrt{3}$ between phase and ground, and $\sqrt{2}\cdot U_{nom}$ between phase and phase, where U_{nom} is the nominal voltage of the system. The 50% flashover voltage, i.e. CFO, $U_{50\%rp}$ at 50 Hz is given in (1) for rod-plane configuration in [8].

$$U_{50\%rp} = 750\sqrt{2} \ln(1 + 0.55D^{1.2}) \text{ [kV peak]} \quad (1)$$

where D is the distance in m.

For the rod-rod configuration, which is typical of the cases under study, standard [8] suggests adopting factors K_{g50} for 50 Hz frequency which is a function of the configuration factor K_{g_sf} for slow front waves and for the same configuration.

$$K_{g50} = K_{g_pf} = 1.35 K_{g_sf} - 0.35 K_{g_sf}^2 \quad (2)$$

$K_{g_sf}=1.60$ for rod-rod configuration, while $K_{g_sf}=1.45$ for rod-structure configuration.

The 50% flashover voltage also depends on environmental conditions (e.g. altitude). This is especially important for the phenomena under study, which occur in case of wet snow events and possibly at not negligible altitudes. To this purpose, the model adopts a very detailed formulation for the environmental derating factor K_a proposed in [9] as in (3).

$$K_a = \delta^m k^w \quad (3)$$

where δ is the air density (depending on air pressure and ambient temperature), while k is a factor equal to

$1+0.012*(h/\delta - 11)$ with h = absolute water vapor density (in g/m^3), in turn a function of the dew point temperature. More details can be found in [10]. Coefficients w and m are calculated from (4).

$$\begin{aligned}\Delta g &= |g - 1.1| \\ w_m &= \max[0, 1.4279 + \Delta g (-4.0689 + \Delta g \cdot (4.5352 - \Delta g * 1.9693))] \\ w &= \min(w_m, 1) \\ m &= \begin{cases} w, & g < 1 \\ 1, & g \geq 1 \end{cases}\end{aligned}\quad (4)$$

where g is the predischarge coefficient given by (5)

$$g = \frac{1.1 U_{\max}}{500 \cdot L \cdot \delta \cdot k} \quad (5)$$

being L the minimum dry arc length in m.

The proposed probabilistic model for the air gap flashover voltage is a Gaussian distribution where the expected value μ_{CFO} is set equal to $U_{50\%} \cdot K_{g50} \cdot K_a$, while the standard deviation σ_{CFO} is chosen so that the probability of flashover is negligible when U_{\max} is applied at standard conditions. Parameter σ_{CFO} also accounts for the higher uncertainty in weather conditions in case of adverse weather conditions. To model these aspects, σ_{CFO} is formulated as in (6).

$$\sigma_{\text{CFO}}(D) = 3\mu_{\text{CFO}}(D) [1 + (1-K_a) \cdot 2] \quad (6)$$

The conditional flashover probability P_{flsh} at peak voltage U_{\max} for a distance D is given by (7).

$$P_{\text{flsh}}(U_{\max}, D) = \Phi(U_{\max}, \mu_{\text{CFO}}(D), \sigma_{\text{CFO}}(D)) \quad (7)$$

D. Modeling the OHL wire spatial configuration

Flashovers can be induced by excessively low distances among phase conductors and shield wires or between phases due to oscillations induced by moderate wind in concurrence with increased sags due to vertical loads of wet snow and differences in the thicknesses of the wet snow sleeves accumulated on wires, depending on the wind profile at the quotes of the wires. Thus, assessing flashover conditions require the knowledge of the spatial positions occupied by OHL span wires. To this purpose, the model is fed with:

- the XYZ positions of the attachment points of wires (both phase conductors and shield wires) of each OHL span.
- The correspondence between each wire and the pair of attachment points at the two terminals of the span.
- The sags computed by the model presented in [4] based on the specific values of wet snow and wind loads.

The model exploits a cylindrical coordinate system based on variables t (distance from one terminal) and γ (inclination angle with respect to vertical line) to mathematically formulate the potential trajectories $X_j(t_j, \gamma_j, F_j)$, $Y_j(t_j, \gamma_j, F_j)$ and $Z_j(t_j, \gamma_j, F_j)$ [6] associated to the j -th wire as in (8).

$$\begin{aligned}X_j(t_j, \gamma_j, F_j) &= x_{1j} + \left[(x_{2j} - x_{1j})t_j + 4\frac{F_j}{l_j} \sin \gamma_j (y_{2j} - y_{1j})(t_j - t_j^2) \right] \\ Y_j(t_j, \gamma_j, F_j) &= y_{1j} + \left[(y_{2j} - y_{1j})t_j + 4\frac{F_j}{l_j} \sin \gamma_j (x_{2j} - x_{1j})(t_j - t_j^2) \right] \\ Z_j(t_j, \gamma_j, F_j) &= z_{1j} + \left[(z_{2j} - z_{1j})t_j + 4F_j \cos \gamma_j (t_j - t_j^2) \right]\end{aligned}\quad (8)$$

being F_j and l_j the sag and the span length for the j -th wire. Reasonable values for variables γ are in the range $(-30^\circ, +30^\circ)$ while variables t are in the range $[0, 1]$.

The next step is to calculate the conditional probability of failure of each OHL span for specified values of the incumbent threat i.e. wet snow linear loads in kg/m . To this purpose, one reasonable assumption is done: at 0 kg/m , i.e. when the threat is not affecting the span, the failure probability of the span is negligible: in fact OHL design criteria are adequate (which is also confirmed by fault statistics).

To this purpose, the model performs the following steps:

- At 0 kg/m , the model evaluates the pairs of (t, γ) for each wire which bring to the minimum distance (between two phases or between one phase and one shield wire) not smaller than the minimum clearance values in air to withstand voltage at industrial frequency reported in TABLE I and in line with the indications from standard EN 50341-1 [8] and. This assures that at 0 kg/m the span does not undergo flashovers.

TABLE I. MINIMUM DIELECTRIC DISTANCE AS A FUNCTION OF THE NOMINAL VOLTAGE, BASED ON [8].

Nominal voltage U_{nom} [kV]	60	132	150	220	400
Clearance distance [m]	0.25	0.4	0.5	0.7	1.2

For the formulation of the problem, two subsets of the initial N_W wires are distinguished: energized wires N_E (i.e. phase conductors) and grounded wires N_{SW} (shield wires), $N_{SW} + N_E = N_W$. Accordingly, two subsets of variables t and γ are defined i.e. $t = [t^{(E)} \ t^{(SW)}]$ and $\gamma = [\gamma^{(E)} \ \gamma^{(SW)}]$. \bar{F}_0 is the vector of the wire sags in case of no snow loads.

The goal is to identify vectors $\bar{t}, \bar{\gamma}$ in order to achieve the lowest distances among the phase conductors and between phase conductors and shield wires, compatible with the fulfillment of the minimum dielectric distance requirement. The optimization problem is in (9) and (10),

$$\arg \min_{\bar{t}, \bar{\gamma}} \left[D_{\min}(\bar{t}, \bar{\gamma}, \bar{F}_0) \right] \quad (9)$$

with

$$\begin{aligned}D_{\min}(\bar{t}, \bar{\gamma}, \bar{F}_0) &= \min \left[D_{\min,E}(\bar{t}^{(E)}, \bar{\gamma}^{(E)}, \bar{F}_0^{(E)}), D_{\min,ESW}(\bar{t}, \bar{\gamma}, \bar{F}_0) \right] \\ D_{\min,E}(\bar{t}^{(E)}, \bar{\gamma}^{(E)}, \bar{F}_0^{(E)}) &= \min_{\substack{i=1 \dots N_E, \\ j=1 \dots N_E, \\ i \neq j}} D_{i,j}([t_i^{(E)} \ t_j^{(E)}], [\gamma_i^{(E)} \ \gamma_j^{(E)}], [F_{0,i}^{(E)} \ F_{0,j}^{(E)}]) \\ D_{\min,ESW}(\bar{t}, \bar{\gamma}, \bar{F}_0) &= \min_{\substack{i=1 \dots N_E, \\ s=1 \dots N_{SW}, \\ i \neq j}} D_{i,s}([t_i^{(E)} \ t_s^{(SW)}], [\gamma_i^{(E)} \ \gamma_s^{(SW)}], [F_{0,i}^{(E)} \ F_{0,s}^{(SW)}])\end{aligned}$$

being $D_{\min,E}$ the minimum distance among the phase conductors, and $D_{\min,ESW}$ the minimum distance between any phase conductor and shield wires.

The problem constraints are given in (10), where D^* is the minimum dielectric distance to be assured according to [8] depending on the nominal voltage of the system.

$$\begin{aligned}D_{\min}(\bar{t}, \bar{\gamma}, \bar{F}_0) &\geq D^* \\ -30 \leq \gamma_w &\leq +30 \quad \forall w = 1 \dots N_W \\ 0 \leq t_w &\leq 1 \quad \forall w = 1 \dots N_W\end{aligned}\quad (10)$$

2. For each linear load $q > 0$ kg/m, wet snow sleeves with thickness d_w accumulate on the wires causing larger sags and wider swings of the wires. Again, the module computes the pairs (t, γ) for each wire which bring to the minimum distance (between two phases or between one phase and one shield wire) not smaller than the minimum values in TABLE I, without considering the sleeve thickness. The problem formulation is similar to the one in step 1 where initial sags in \bar{F}_0 are replaced with the increased sags at load q in vector \bar{F}_q . Given the configuration of pairs (t, γ) solving this problem, the model computes the actual distances D by subtracting the corresponding sleeve thicknesses to the distances coming from the problem solution and computes the probabilities of flashover $P_{\text{flsh}}(U_{\max}, D)$ based on equation (7) in subsection II.C. The maximum flashover probability is also the conditional probability of OHL span failure due to reduced insulation distance for any wet snow load q .

Constraint (10) assures the compliance with the minimum dielectric distance in case of no snow loads, which is a reasonable assumption. The analogous constraint in step 2, in case of increased sags due to wet snow loads, is set to avoid overestimating the vulnerability of the OHL span to flashover, especially in case of low wet snow loads. The main goal of such constraints is to increase the robustness of the model: in fact, without these constraints, small errors in the spatial positions of the wire attachment points would lead to strong under- and over-estimation of failure probabilities; in addition, many environmental aspects (e.g. wind speed and direction) depend on the specific event (not known a-priori) and -anyway- are affected by large uncertainties. The optimization problems in steps 1 and 2 only verify the existence of a minimum distance equal to the minimum dielectric distance requirement, given the wire sags and sleeve thicknesses associated to each linear wet snow load: this verification is much less sensitive to potential uncertainties in the XYZ positions of the wires and environmental conditions. An interesting outcome from solving the formulated optimization problems in both steps is the identification of the distance and the relevant configuration (phase-shield wire or phase-phase) associated with the highest flashover probability for each wet snow load q : this implies the ability of the model to discriminate between flashovers among phase conductors (leading to two-phase faults) from flashovers between phases and shield wires (leading to one-phase to ground faults).

E. Model use in resilience assessment analyses

The vulnerability curves computed using the proposed model are combined with the climate curves, which represent the probability of overcoming specific values of linear wet snow loads in a climatological period (e.g. a future horizon 2020-2030 or a reconstructed past climatological period) in the methodology described in [11] in order to compute the return periods (RP) for the outages of the grid asset (specifically lines). The methodology has been developed in collaboration with the Italian TSO and it is used to compute long term resilience indicators with the final aim to prioritize the interventions in the annual resilience plan of the TSO. More details on the methodology and its validation are given in [11].

III. THE CASE STUDY

The present section discusses the results of the application of the proposed vulnerability model.

A. Test system and simulation scenarios

The test system under test is a portion of the Italian EHV and HV transmission grid with a focus on a small set of 6 lines (three at 132 and three at 60 kV) located in an area particularly subject to frequent OHL flashovers in concurrence with moderate wet snow events. The simulation scenarios are summed up in TABLE II. In simulation case SEL the data feeding the model consist in the XYZ positions of attachment points of the wires of each OHL spans, detected with a good accuracy by a Lidar (Light Detection and Ranging) system available at TERNA.

TABLE II. SUMMARY OF THE SIMULATION SCENARIOS.

Sim ID	Description	Goal
SEL	Compute the vulnerability curves for the spans of the 6 lines of the test set using complete information (absolute XYZ positions of attachment points), compare the relevant outage RPs with the statistics from past recorded fault events.	Testing the selectivity of the model
ROB	Compute the same vulnerability curves using incomplete information (relative positions of attachment points in the tower transversal plane).	Testing the model robustness

In simulation case ROB, instead of the accurate data from Lidar detection of the OHL wires, the model is fed with a smaller amount of data estimated from available information on towers, consisting in the relative position of the same attachment points in the transversal plane of each tower support, representing only the distance of each point from the central axis of each support and the height of the same point with respect to the ground.

The validation process consists in the following steps:

- the vulnerability curves computed using the proposed model are combined with the climate curves which represent the probability of overcoming specific values of linear wet snow loads in a climatological period (typically 2010-2020) according to the methodology in [4] to get the outage RPs of the lines,
- the “failure rate” λ_a over the 2010-2020 period expressed as the inverse of the analytical RPs at step 1 are compared with the failure rate λ_e due to flashovers on the same set of lines estimated as n_e/T , where n_e is the number of recorded fault events in $T = 10$ years from 2010 to 2020. The counting of the faults for statistical analyses follows the following assumptions: (a) only events with recovery durations longer than 10 minutes are counted, (b) multiple faults on the same lines in the same weather event are considered as one single event.

B. SEL simulation case: proof of the model selectivity

TABLE III compares the analytical RPs, the relevant failure rate λ_a and the empirical failure rate λ_e . First of all, the comparison of the first two columns (in particular, the strong RP reduction on lines 4, 5 and 6) highlights the importance of including the proposed model to catch the recorded faults concerning the reduced insulation distances in presence of wet snows. It’s worth noting that lines 4 and 5, exhibiting the lowest analytical RPs (8.80 and 2.63 years), have also the

highest empirical failure rates (respectively 0.11 and 0.38 #faults/yr) due to flashovers for reduced insulation distances. Other lines (such as lines 1 thru 3 at 132 kV and line 6 at 60 kV), although located in the same geographical area, are characterized by very few or no faults in the 10 years of operational practice: this is also captured by the model, which attributes very high analytical RPs to these lines. This proves the selectivity of the model which takes into account not only the environmental features of the area but also the specific geometrical configurations of the lines. As expected, the lines with the highest failure rates are characterised by the lowest voltage level 60 kV (both in the analytical model and in the statistics of recorded faults).

TABLE III. ANALYTICAL MODEL OUTCOMES (RPS AND FAILURE RATES) WITH EMPIRICAL FAILURE RATES, SEL SIMULATION CASE.

Line ID	Analytical RPs without proposed model (yr)	Analytical RPs with proposed model (yr)	Analytical failure rate with proposed model, λ_a (# faults/yr)	Empirical failure rate, λ_e (# faults/yr)
Line 1 (150 kV)	781	313	0.003199	0
Line 2 (150 kV)	1199	219	0.004565	0
Line 3 (150 kV)	318	317	0.003155	0
Line 4 (60 kV)	361	8.80	0.11366	0.1
Line 5 (60 kV)	605	2.63	0.379856	0.4
Line 6 (60 kV)	237	62	0.016129	0

Line 6 at low voltage level (60 kV) shows a lower failure rate with respect to lines 4 and 5: the reason lies in the lower number of spans for line 6 and in larger spacings -on average- among the wires with respect to lines 4 and 5, which implies larger clearance distances, but also in the lower probabilities of wet snow events (the average probability of wet snow loads higher than 1 kg/m in the OHL spans passes from 54% and 90% for lines 4 and 5 to 1.5% for line 6): all these factors lead to lower flashover probabilities for line 6. The solution of the optimization problem for line 5 indicates the reduced distance between two phase conductors as the cause of flashover, which is confirmed by fault records indicating multi-phase faults during the events recorded on line 5 over 10 years.

C. ROB simulation case: proof of the model robustness

This simulation consists in running the same model as the SEL case, using a more restricted amount of data, i.e. the relative positions of the attachment points instead of their absolute XYZ positions. This implies a lower degree of accuracy in locating the wire: this situation can occur in practice in those cases when no updated Lidar information are available. TABLE IV compares the analytical RPs computed with the full set of available information (SEL simulation case) and the more limited set of data (ROB simulation case).

TABLE IV. ANALYTICAL OUTAGE RPS WITH FULL INFORMATION SET (2ND COLUMN) AND PARTIAL INFORMATION SET (3RD COLUMN), ROB SIMULATION CASE.

Line ID	Analytical RPs with full information (yr)	Analytical RPs with partial information (yr)
Line 1 (150 kV)	313	205
Line 2 (150 kV)	219	332
Line 3 (150 kV)	317	257
Line 4 (60 kV)	8.80	3.02
Line 5 (60 kV)	2.63	1.76
Line 6 (60 kV)	62	74

It's worth noting that the lack of updated data in this simulation scenario does not significantly affect the capability of the tool in detecting the most "vulnerable" lines: in fact, still

lines 4 and 5 at 60 kV show the lowest RP's among the line set. The main effects of the partial information set consist in a slight overestimation of the failure rates for lines 4 and 5, whose outage RPs pass from 8.80 and 2.63 yr to 3.02 and 1.76 yr, as well as an underestimation of failure rate for line 6.

IV. CONCLUSION

The paper has proposed an analytical model for the quantification of the vulnerability of the wires of OHL spans to flashovers induced by concurrent causes (wind induced wire swinging and increased sags due to vertical loads for wet snow events). The model accounts for both environmental aspects (altitude, orography, temperature and air pressure) and geometrical aspects concerning the spatial trajectories potentially drawn by span wires during the application of the concurrent threats. The application case study on a small set of OHLs in a portion of the Italian EHV/HV Italian transmission grid affected by frequent flashovers shows that the model is selective i.e. able to select exclusively the lines which have undergone recorded faults in the last decade. Moreover, the adoption of a smaller amount of data does not affect the results in a significant way, which is important for a potentially extensive application of the model even in those areas where Lidar data are available with lower updating rates. Further work consists in an extensive application of the promising model to larger sets of lines.

ACKNOWLEDGMENT

This work has been financed by the Research Fund for the Italian Electrical System under the Three-Year Research Plan 2022-2024 (DM MITE n. 337, 15.09.2022), in compliance with the Decree of April 16th, 2018.

REFERENCES

- [1] M. Panteli, P. Mancarella, "Influence of extreme weather and climate change on the resilience of power systems: Impacts and possible mitigation strategies", *El. Power Systems Research*, Elsevier, Vol. 127, 2015, pp. 259-270.
- [2] K. Finch e C. Allen, "Understanding Tree Caused Outages", in EEI Natural Resource Conference, Palm Springs, CA, April 2001.
- [3] T. Todic, P.C. Chen, M. Kezunovic, "Risk Analysis for Assessment of Vegetation Impact on Outages in Electric Power Systems", CIGRE US National Committee Symposium, 2016.
- [4] E. Ciapessoni, D. Cirio, G. Pirovano, A. Pitto, F. Marzullo, A. Lazzarini, F. Falorni, F. Scavo, "Modeling the overhead line vulnerability to combined wind and snow loads for resilience assessment studies," *2021 IEEE Madrid PowerTech*, Madrid, Spain, 2021, pp. 1-6, doi: 10.1109/PowerTech46648.2021.9494913.
- [5] TERNA, "Qualità del servizio di trasmissione - Rapporto annuale per l'anno 2019", Annual Report (in Italian), 2019.
- [6] W. Huang, J. Zhu, Z. Du, Z. Zhang, "Calculation of the Two High Voltage Transmission Line Conductors' Minimum Distance". *World Journal of Engineering and Technology*, Vol 3, 2015, pp. 89-96. doi: [10.4236/wjet.2015.33C014](https://doi.org/10.4236/wjet.2015.33C014)
- [7] Zhou, C.; Yin, J.; Liu, Y. Large Swing Behavior of Overhead Transmission Lines under Rain-Load Conditions. *Energies* 2018, *11*, 1092. <https://doi.org/10.3390/en11051092>
- [8] CEI EN 50341-1:2013-10, "Overhead electrical lines exceeding AC 1 kV - Part 1: General requirements - Common specifications", 2013.
- [9] CEI (Italian Electrotechnical Committee) Std 11-4, "Norme tecniche per la costruzione di linee elettriche aeree esterne" (in Italian), 1998-9.
- [10] IEEE standard 4, *IEEE standard techniques for high voltage testing*, Piscataway, IEEE press, 1995.
- [11] E. Ciapessoni, D. Cirio, A. Pitto, E. Ferrario, M. Lacavalla, P. Marcacci, G. Pirovano, F. Marzullo, F. Falorni, A. Lazzarini, F. Scavo, S. Costa, S. Pierazzo, C. Vergine, "Validation and application of the methodology to compute resilience indicators in the Italian EHV transmission system", 2022 CIGRE Session, Aug 28-Sept 2, 2022, Paris, p. 1-14.